



## Transgressive coastal systems (2<sup>nd</sup> part): geometric principles of stratal preservation on gently sloping continental shelves

Paolo Tortora\*, Peter John Cowell\*\*, Kellie Adlam\*\*

\*Dipartimento di Scienze della Terra, SAPIENZA Università di Roma, P.le A. Moro, 5 - 00185 Roma, Italy

\*\*School of Geosciences, University of Sydney Institute of Marine Science, NSW 2006 Australia

**ABSTRACT** - This study focuses on the causes and mechanisms of coastal-lithosome preservation during transgressions driven by roll-over processes of barrier migration. Using the Shoreface Translation Model, a large range of idealised coastal settings was simulated to identify the environmental conditions of stratal preservation. Preservation occurs within two broad categories of experimental conditions. The first category relates to transgressive phases evolving under relatively constant conditions in which stratal preservation takes place only if the coastal barrier experiences positive net sediment supplies. The resulting deposits show tabular geometries, have poorly differentiated internal architectures and tend to extend continuously with quite uniform thickness upslope across plain regions of the shelf. In the second category, by comparison, deposits are thicker and stratal preservation is more localised. Moreover preservation occurs as an adaptive morpho-kinematic response to environmental perturbations due to variations in: (1) the ratio of sediment supply ( $V_s$ ) to accommodation generated by sea-level rise (SLR); (2) the substrate topography; (3) the morphology of the barrier profile. More specifically, changes of the ratio  $V_s$  /SLR, where SLR is an approximate surrogate for added accommodation space, directly promotes growth of the barrier ( $V_s$  /SLR  $\gg$  0) and its subsequent drowning ( $V_s$  /SLR  $\rightarrow$  0). The topographic variations of the substrate may include minor irregularities as well as sudden changes in gradient that afford other types of preservation, such as local fills and residual littoral packages. Finally, barrier-profile changes inducing stratal preservation may include the reduction in barrier width and depth of surf base as well as the increment in shoreface concavity and shoreface length. Simplified methods are given for relating the geometry of preserved deposits to rates of sea-level rise and sediment supply over different shelf slopes, and for identifying the position of the shoreline at specific times. Holocene evolution of some coastal deposits from the Tuscan shelf (Italy) is presented in a morpho-kinematic reconstruction to illustrate the geometric relationships for stratal preservation.

**KEY WORDS:** coastal system, sea level rise, stratal preservation, kinematic models

Submitted: 17 february 2009 - Accepted: 31 july 2009

### INTRODUCTION

This study examines the causes and mechanisms of coastal lithosome preservation during transgressions driven by roll-over processes (Dean and Maurmeyer, 1983; Leatherman, 1983; Cowell et al., 1999). Roll-over processes entail the continual reworking of sediments from the entire shoreface to the subaerial components of the coastal system (beach and back-barrier), allowing the barrier to be regenerated landwards of its original position and thus to migrate over the antecedent topography (Tortora et al., 2009, in this volume). Preservation refers to the portion of the barrier which is not transferred landwards and which, due to sea-level rise, is cut off from the coastal zone and potentially buried on the continental shelf (Heward, 1981; Belknap and Kraft, 1981; 1985).

The objective of the study was to explore conditions favourable to strata preservation under two broad sets of conditions: relatively constant and highly variable transgressive environments. The approach involved analysis of hypothetical cases synthetically generated by the Shoreface Translation Model (STM). This model, given the appropriate environmental parameters (input data), outputs the kinematics of barrier migration and the resulting morpho-stratigraphic effects in terms of a series of geo-

metric forms recorded at equal time intervals along the land-sea profile (Cowell et al., 1995).

Relevant characteristics of the STM, and details of roll-over migration and the experimental techniques used, have all been covered in Tortora et al. (2009, in this volume) and other works relating to the theory and application of the STM or similar models (Cowell and Roy, 1988; Dean, 1991; Thorne and Swift, 1991; Cowell et al., 1992; Cowell and Thom, 1994; Niedoroda et al., 1995; Stive and De Vriend, 1995; Cowell et al., 1999; Dillenburg et al., 2000; Kench and Cowell, 2001; Cowell et al., 2003a; 2003b).

### BASIC CONCEPTS

Effects of sea level-rise are illustrated in Fig. 1 by comparing typical stratigraphic evidence of the transgression (in A) with a much simplified schematisation of kinematic reconstructions using the STM (in B). Both the illustrations show a coastal cell experiencing roll-over processes, by which the sediment previously eroded from the full length of the shoreface (cut) is redeposited on the subaerial barrier portion (fill). In A, the products of this redeposition are represented by the stratigraphic column 1, whilst the column 3 shows a preserved barrier portion affected by the cut in the earlier phase. Stratigraphic-columns 2, 4 and 5, are alternative columns to the third one. Therefore columns 2 through 5 idealise the possible transformations that the original barrier

\*Corresponding author: [paolo.tortora@uniroma1.it](mailto:paolo.tortora@uniroma1.it)

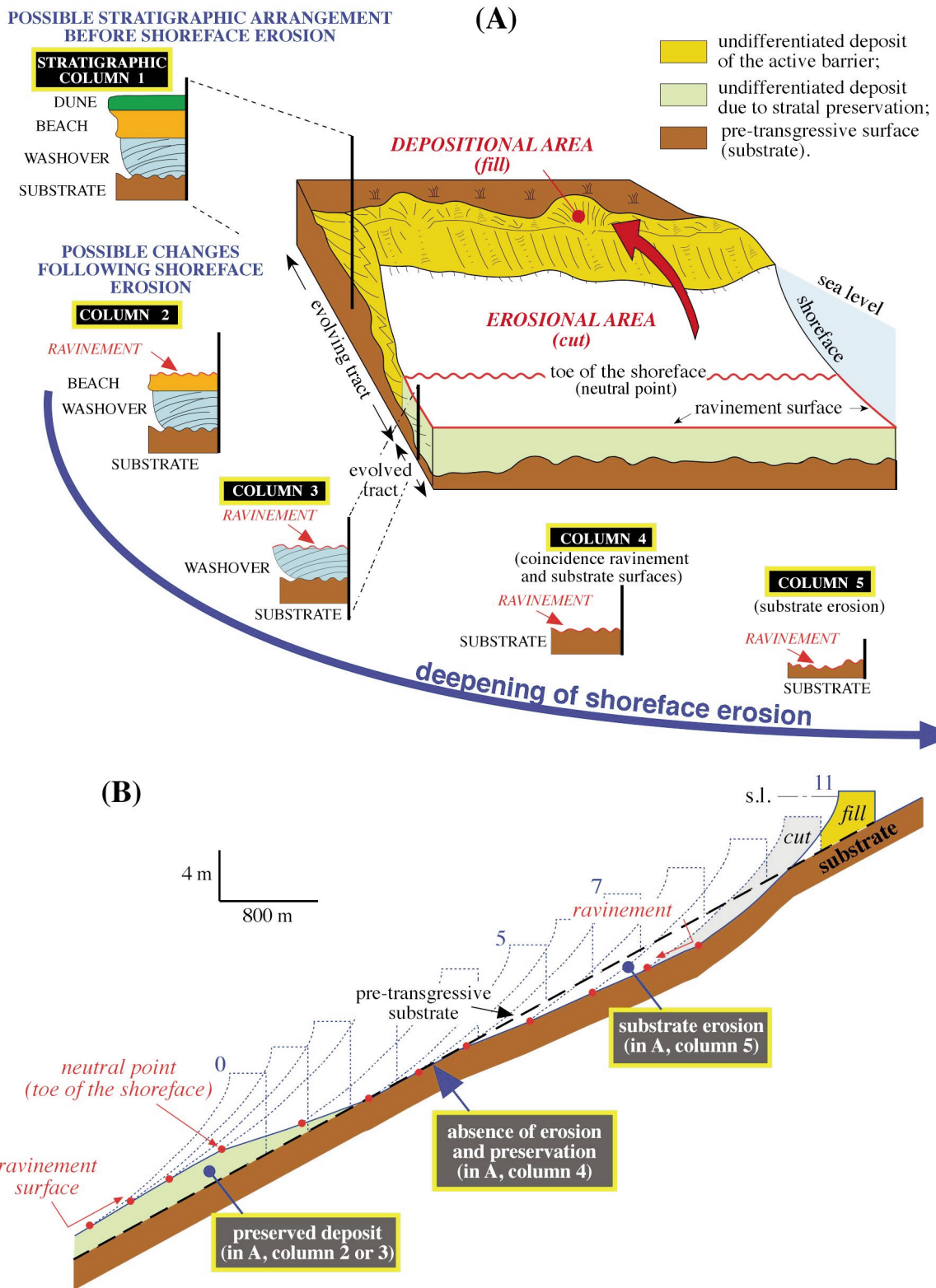


Fig. 1 - Differences in stratal preservation due to variations in coastal accommodation during sea-level rise. In A, littoral cell with typical barrier roll-over in cross-section, in which sediments eroded on the shoreface (cut) are redeposited (fill) onto the emerged coast to produce the stratigraphy 1. Columns 2 through 5 idealise the possible transformations of the original barrier (stratigraphy 1) depending on changes in depth of shoreface erosion (cut) during transgression. In B, kinematic transformations from STM simulation for stratal columns 2 (or 3), 4 and 5 respectively generated at time-step intervals 0-5, 5-7 and 7-11.

(as shown in column 1) could undergo as the transgression proceeds: as erosion reaches to greater depths, the preservation potential decreases becoming zero as it reaches

or even penetrates the substrate (column 4 and 5). For preservation to occur, shoreface erosion must be contained somewhere between two levels: the barrier top (total

preservation) and immediately above the substrate (minimal preservation). The facies within the preserved deposit also depend on the depth of erosion (Heward, 1981; Boyd and Penland, 1984; Tortora et al., 2001).

Figure 1B shows the preservation kinematics of the stratigraphic columns in Fig. 1A. The initial phase of evolution (steps 0-5) may be regarded as corresponding to column 2 or 3, the intermediate phase (steps 5-7) to column number 4, and the final phase (steps 7-10) to column 5. These three phases depend on the neutral point: the point on the shoreface that corresponds to the depth of the surf base driving the erosion, which, in rollover-type barrier migrations, is the depth at the toe of the shoreface (Tortora et al., 2009). These three phases depend on the trajectory traced by the neutral point during sea-level rise: whether the trajectory (i.e. ravinement surface) lies above the substrate (steps 0-5), corresponds to (steps 5-7), or lies below it (7-10). In the illustrated experiment, the trajectory is governed by the sediment input ( $V_s$ ) to the coastal cell (successively,  $V_s > 0$ ,  $V_s = 0$ ,  $V_s < 0$  m<sup>3</sup>).

The preserved deposits (steps 0-5) are therefore bound from above by the ravinement surface and from below by the substrate (paleotopography). The vertical distance between the ravinement and substrate determines the degree of stratal preservation (Belknap and Kraft, 1981, 1985). Such deposits, defined as inland dispersal systems deposits (Swift et al., 1991), include remnants of the original redeposition on the back-barrier (column 1 in Fig. 1A, the fill in Fig. 1B) and generally derive from overwash, aeolian and flood tidal delta processes (Roy et al., 1994; Tortora, 1996).

## PRESERVATION OF COASTAL DEPOSITS UNDER RELATIVELY CONSTANT CONDITIONS

### Control factors

Constant conditions mean that the following control factors remain relatively stable during a transgressive phase: sea-level rise (SLR); sediment budget ( $V_s$ ); substrate gradient ( $\alpha$ ); morphological profile of the barrier ( $M$ ). Under relatively stable conditions, the preservation of coastal lithosomes is possible only if the transgression receives a positive sediment supply ( $V_s > 0$ ), as indicated in the four examples of Fig. 2 in which the only parameter to differ between cases is  $V_s$ . In A and B, trajectories of the neutral point (respectively of 0.77° and 0.48°) are steeper than the substrate slope (0.3°), resulting in stratal preservation. In C, the gradient of the trajectory is the same as the substrate slope, producing neither preservation nor erosion. In D, the trajectory (0.23°) is lower than the substrate slope, causing substrate erosion (Roy et al., 1994; Wolinsky and Murray, 2009). Only cases with positive net sediment input ( $V_s$ ) produce stratal preservation (Fig. 2A and B). The trajectory of the neutral point traces the ravinement surface (Tortora et al., 2009).

Overall, the simulations in Fig. 2 demonstrate how  $V_s$  controls the translation of the barrier (increasing from A to D), the trajectory of barrier migration (becoming less steep from A to D), and therefore also the path traced by the neutral point (ravinement surface), limiting stratal preservation to A and B. Extending these four cases over additional time steps would result in phases of roll-over transgression defined as depositional (A and B), neutral (C) and erosive (D) types (Cowell et al., 1995; Tortora et al., 2009). Under relatively constant conditions, therefore, stratal preservation may only occur during depositional roll-over ( $V_s > 0$ ).

The resulting deposits differ in geometry as a function of SLR,  $+V_s$  and  $\alpha$ , according to the degree of control exerted by each on the coastal system. This individual control can be inferred from Fig. 3 by comparing case A with each of the other cases in turn, which differ from A only through lower values of SLR (B),  $V_s$  (C) and  $\alpha$  (D). A comparison of the preserved deposits shows that their geometry depends upon the migration path of the barrier (particularly the neutral point), and on how this path is controlled by each parameter. Results from variation in the control variables were quantified using tracking parameters introduced in Tortora et al. (2009). With reduced rates of SLR (compare A and B), the trajectory becomes steeper (in B) and the deposit has a greater thickness ( $S$ ) but a smaller volume ( $V_p$ ) and land-sea extension (equal to the total translation distance,  $A_r$ ). The parameters  $V_s$  and  $\alpha$  have the same effect (compare A-C, and A-D in Fig. 3): a reduction in either is accompanied by a trajectory path of reduced steepness, with lower thickness and volume (only for case C) of the preserved mass which, however, is spread further along the profile.

The geometry of the preserved deposit, nevertheless, actually depends on the combination of all three parameters, SLR,  $V_s$  and  $\alpha$ . Relations between these variables and some geometric elements within the barrier (Fig. 4), allow prediction of the length (equal to the translation distance,  $A_r$ ) and thickness ( $S$ ) of the preserved deposit along

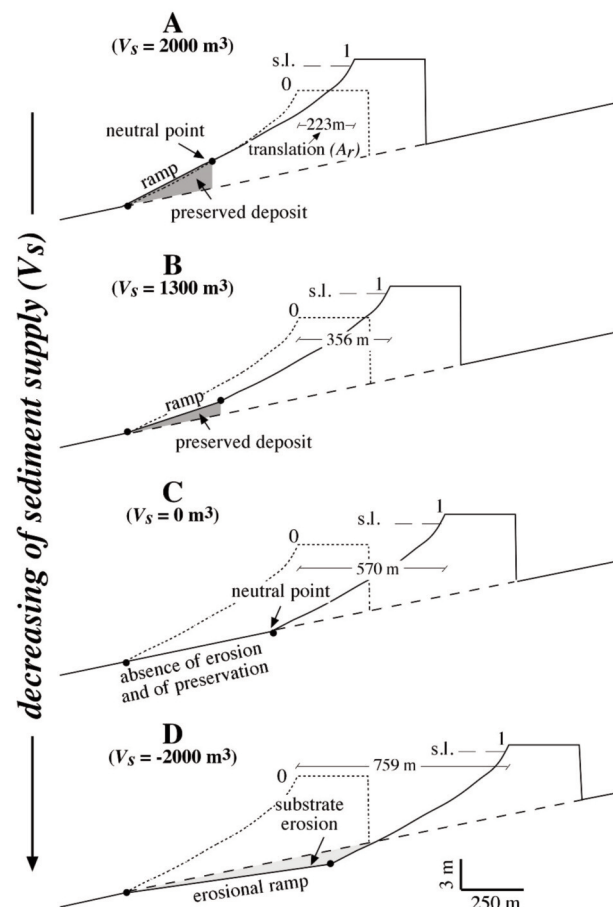


Fig. 2 - Simplified examples showing the influence of sediment supply ( $V_s$ ) on the trajectory of the neutral point upon which stratal preservation depends: (A) over-supplied system,  $V_s > 0$ ; (B) over-supplied system  $V_s > 0$ ; (C) closed or balanced system,  $V_s = 0$ ; (D) depleted system,  $V_s < 0$ .



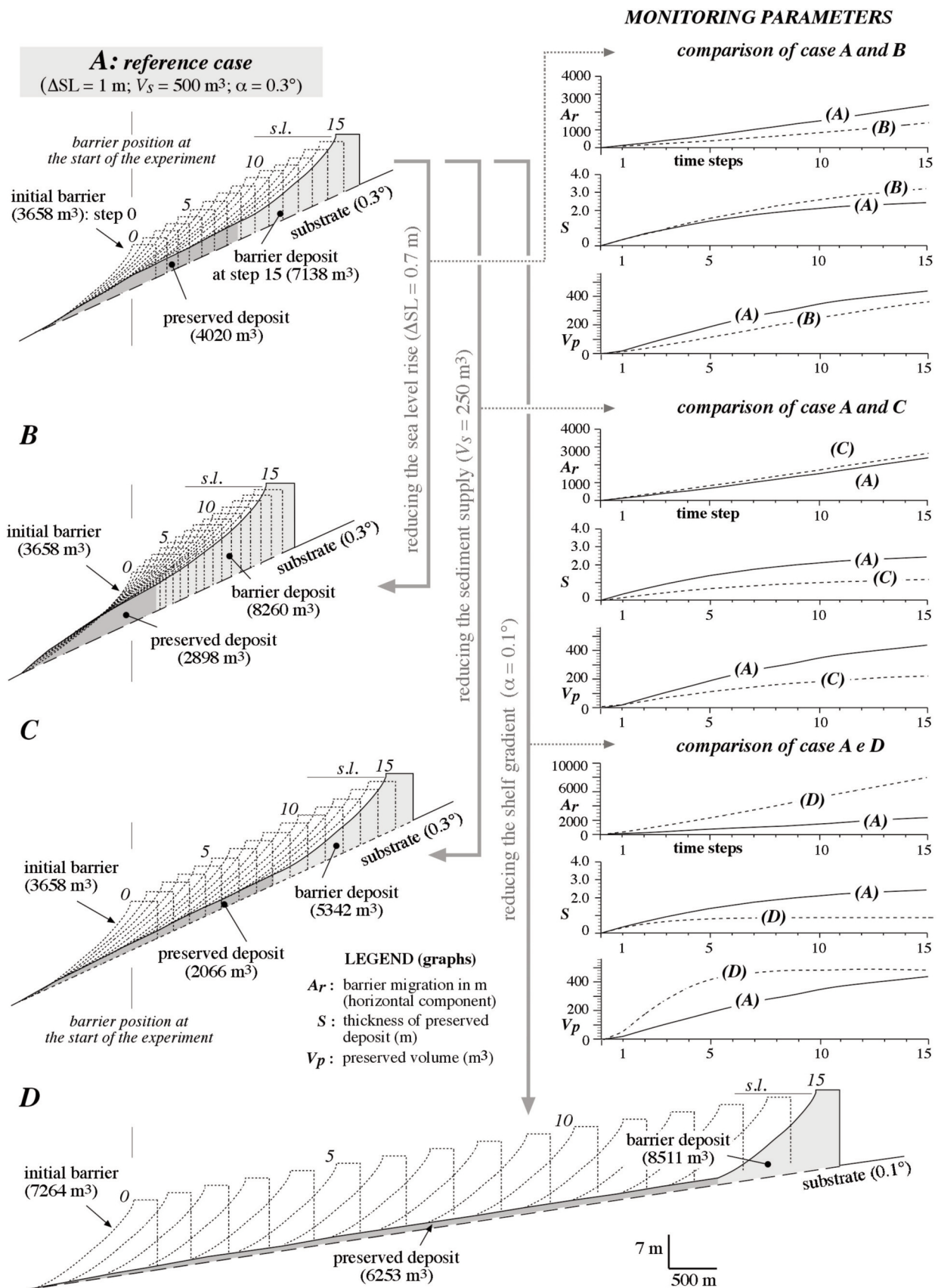


Fig. 3 - Comparative effects of governing variables (SLR,  $V_s$ ,  $\alpha$ ) on stratal-preservation: (A) reference case; (B) lower SLR than ref. case; (C) lower sediment supply ( $V_s$ ); (D) lower substrate slope ( $\alpha$ ). Graphs to right show time variation in stratal-preservation tracking parameters: littoral translation ( $A_r$ ), thickness ( $S$ ) and volume ( $V_p$ ) of the preserved deposits.



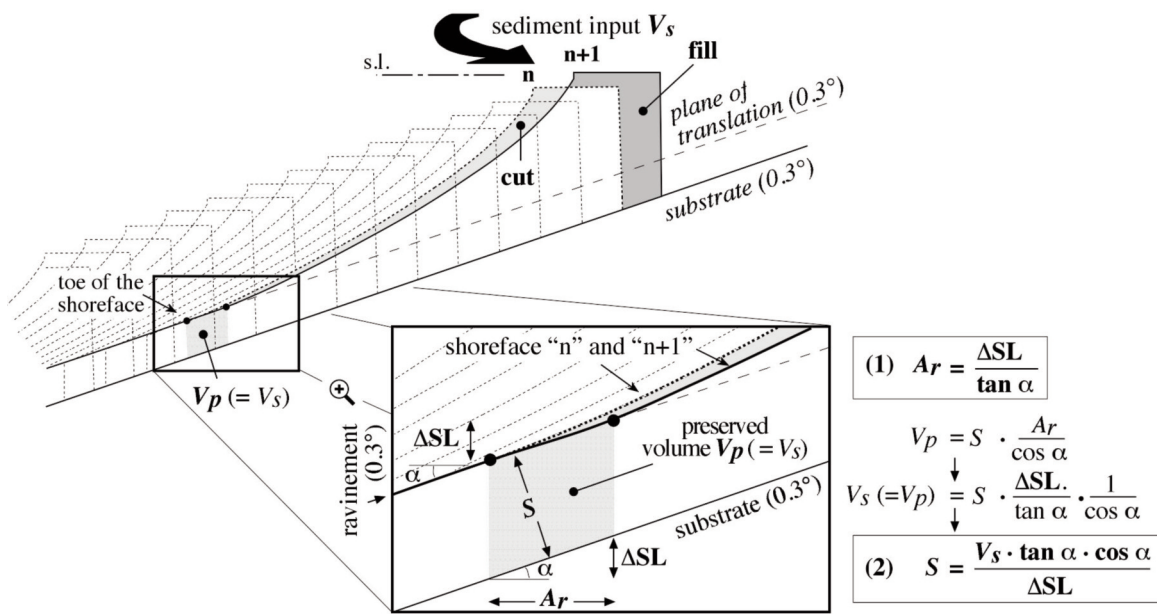


Fig. 4 - Schematics and equations for geometric relationships under steady state conditions (see text for definition of variables).

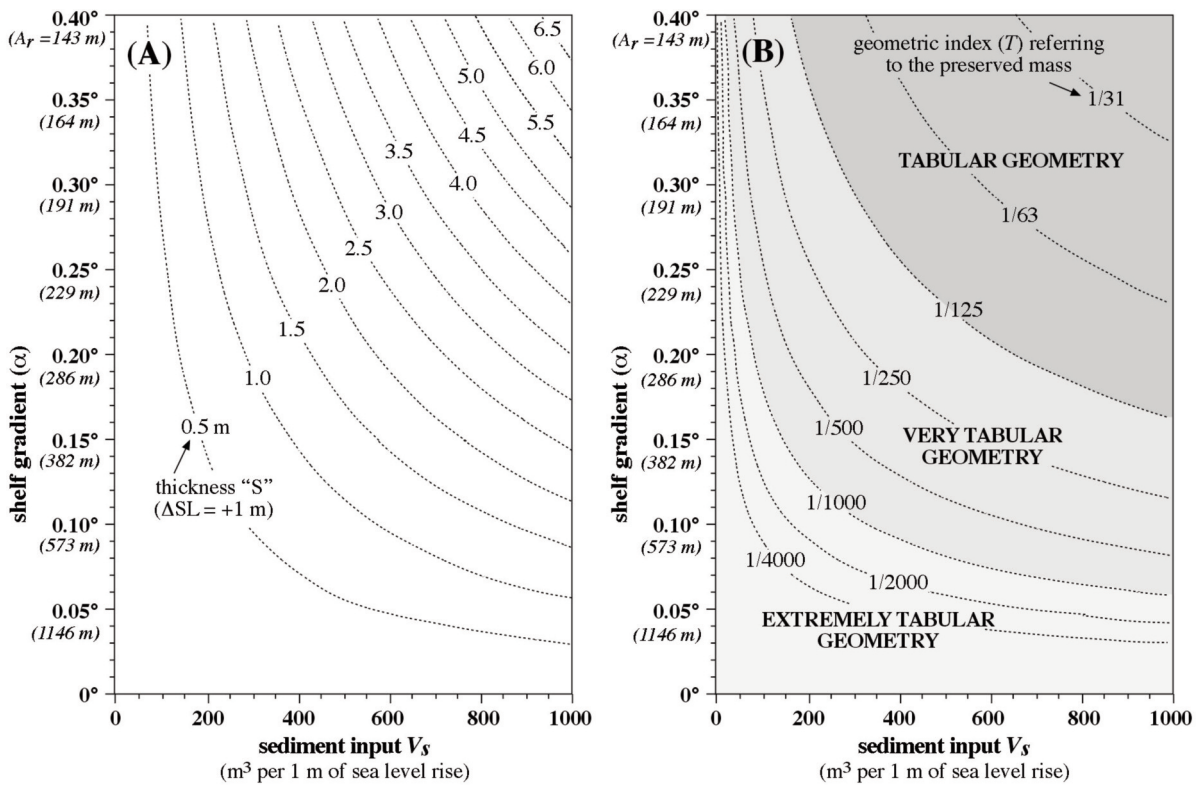


Fig. 5 - Reference charts to predict properties of preserved strata (values of tracking parameters  $A_r$ ,  $S$ ,  $T$ ), per metre of SLR, as a function of governing variables ( $V_s$  and  $\alpha$ ) for depositional roll-over types under morpho-kinematic steady-state conditions: (A) thickness of preserved deposit; (B) tabularity index.

the profile for any roll-over, even erosional ( $A_r$  and  $-S$  signify extension and depth of the substrate cut). These relations are only valid once kinematic equilibrium has been attained under constant conditions (Tortora et al., 2009). That occurs when the barrier migration is no longer affected by kinematic inertia or, in other words, when continued evolution entails invariant processes and geological products due to the balance between sediment input and mass lost on the shelf from stratal preservation (Fig. 4). Then,

the geometric parameters  $A_r$  and  $S$  can be estimated from any set of governing variables (SLR,  $V_s$ ,  $\alpha$ ), or viceversa:

$$A_r = SLR / \tan \alpha \quad (1)$$

and

$$S = (V_s \tan \alpha \cos \alpha) / SLR \quad (2)$$

These equations yield solutions for  $S$  plotted per unit SLR (Fig. 5A), showing how the thickness ( $S$ ) and the extension

( $A_r$ ; in brackets on the vertical axis) of the deposit vary as a function of the net sediment input and substrate gradient. From this it can be inferred that deposits tens of cm thick with pronounced longitudinal extension would result on sub-horizontal shelves, and would therefore only include the lower portion of the original coastal stratigraphy (lower portion of column 1, Fig. 1A). Thus the geometry of the preserved deposits, quantified by the tabular index,

$$T = S/A_r \cos \alpha \quad (3)$$

becomes flatter (more tabular) with reduction in sediment supply and shelf gradient (Fig. 5B). Note the strong control of the latter on the extension  $A_r$  (vertical axis): e.g.  $A_r = 1146$  m for  $\alpha = 0.05^\circ$  compared to  $A_r = 143$  m for  $\alpha = 0.4^\circ$ .

### Determining age by geometric extrapolation

Figure 6 shows several steps of a depositional roll-over evolution ( $V_s > 0$ ). The following concerns stratal preservation, specifically the deposit of column  $P_1$  formed at time step 0,

and the ravinement surface above it formed at step 1. Calculations based on geometric rules allow their respective formation ages and the position of their associated coastlines to be determined. The method requires measurements taken from the relevant stratigraphic section (the preserved deposit in Fig. 6) plus some of the parameters (if only hypothetically) of the transgressive barrier ( $L_n, h_n, W_*$ ); a sea-level rise curve is also required.

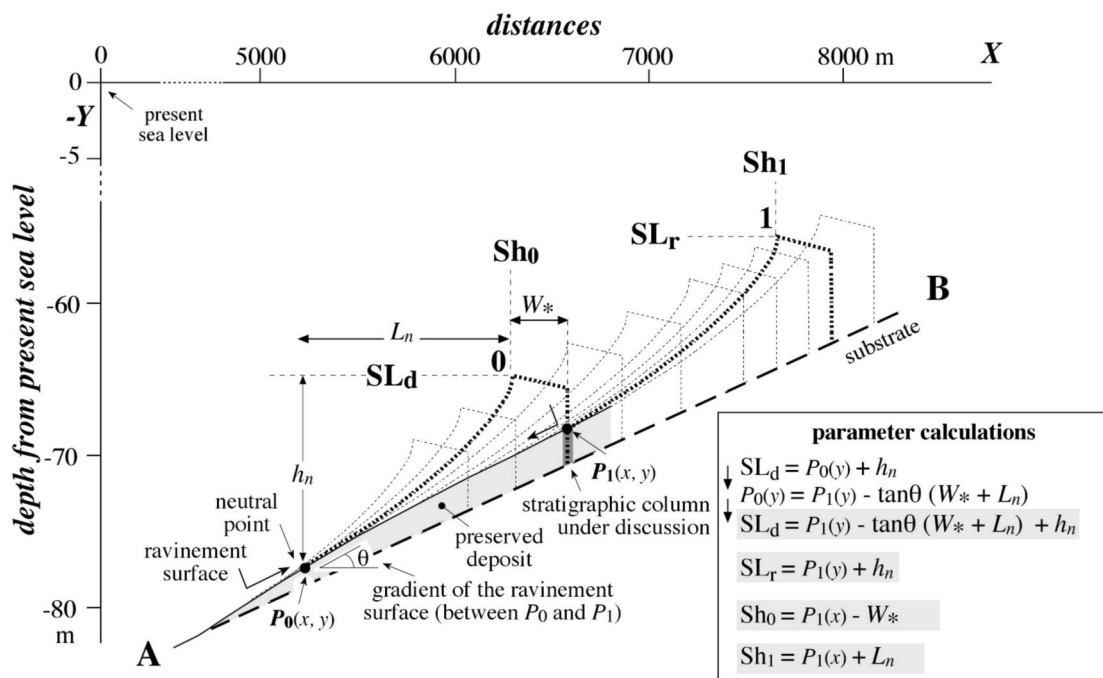
Following this example, the two ages (deposition and preservation of column  $P_1$ ) can be calculated, using the eustatic curve, from sea-level (SL) estimates related to deposition of the column  $P_1$  ( $SL_d$ ) and to the formation of the overlying ravinement surface ( $SL_r$ ):

$$SL_d = P_1(y) + h_n - \tan \theta (W_* + L_n) \quad (4)$$

and

$$SL_r = P_1(y) + h_n \quad (5)$$

where,  $P_1(y)$  is the depth of the top of the column with respect to the present sea level,  $\theta$  is the slope of the



data for calculations		data obtained from calculations	
<i>measurements taken from section A-B:</i>			
$P_1(x, y)$	coordinates of the stratigraphic column (in dark grey) from which the formation age (step 0) may be deduced as well as that of the ravinement surface above it (step 1)	$P_0(x, y)$	coordinates of the neutral point (toe of the shoreface) relative to the barrier at step 0
$\theta^\circ$	gradient of ravinement surface in the tract between $P_1(x)$ and $P_1(x) - (W_* + L_n)$	$SL_d$	sea level (step 0) during the deposition of the stratigraphic column under $P_1$
<i>estimated measurements:</i>			
$W_*$	assumed width of the emerged barrier	$SL_r$	sea level (step 1) during formation of the ravinement surface at point $P_1$ (above the stratigraphic column)
$L_n$	assumed distance from shoreline to the neutral point (located at the toe of the shoreface: on $P_0$ and $P_1$ )	$Sh_0$	position of the shoreline associated to $SL_d$
$h_n$	assumed water depth (assigned a negative value) of the neutral point (toe of the shoreface)	$Sh_1$	position of the shoreline associated to $SL_r$

Fig. 6 - Schematic relations for method to define formation age of a relict roll-over deposit (column  $P_1$ ) and the ravinement surface at its top, with location of the respective shorelines.

ravinement surface (between  $P_0$  and  $P_1$ ),  $W_*$  is the assumed width of the emerged barrier,  $L_n$  is the distance from the shoreline to the neutral point (the toe of the shoreface),  $h_n$  is the original water depth of the neutral point ( $h_n > 0$  following the usual convention).

The positions of the respective shorelines (during deposition and preservation of column  $P_1$ ) have  $y$ -coordinates equal to sea levels  $SL_d$  and  $SL_r$  previously estimated, and  $x$ -coordinates:

$$Sh_0 = P_1(x) - W_* \quad (6)$$

and

$$Sh_1 = P_1(x) + L_n \quad (7)$$

This method is applicable to extensive shore-perpendicular stratigraphic sections (typically seismic lines), and to Holocene transgressions in which the SL record (i.e. the eustatic curve) is more detailed and the vertical disturbances following deposition, such as tectonics and subsidence, are generally minimal. This method is also valid for neutral and erosional roll-over processes. In such cases it yields ages related to the formation of a barrier deposit and to its subsequent total erosion by the shoreface migration. Only the second age is linked in any way to comparable stratigraphic effects (the ravinement-surface formation).

Extrapolation of this approach allows its spatial application on continental shelves where evidence of all three roll-over types might co-exist. Thus, using equations (5) and (7), it is possible to generate a dated sequence of transgressive coastline positions. For example, assuming the availability of grid data to describe the topography of the ravinement surface (depths from present SL), the procedure involves four steps: (1) using an available eustatic curve, extract the sea-level sequence corresponding to the preselected temporal series of coastline positions to be mapped (e.g. a SL measurement every 300 years); (2) deepen this sea-level sequence by the value of  $h_n$ ; (3) and then contour it from the topographic grid data (ravinement surface); (4) translate the resulting contour-line landwards (in the same direction as the transgression) by the  $L_n$  value. The contour-lines in point (3) and (4) respectively indicate, for the preselected temporal series, where the shoreface erosion occurred (i.e. the location of the neutral point) and, finally, the position of the associated shoreline.

Note that the cases for which this method is intended (roll-over in relatively constant conditions),  $L_n$  and  $h_n$  are relatively easy to calculate, because the neutral point is always anchored to the toe of the shoreface. The method is also applicable to non roll-over transgressions - hybrid and encroachment modes of barrier migration (Tortora et al., 2009) - if the parameters of the neutral point ( $h_n$  and  $L_n$ ) are known.

### PRESERVATION OF COASTAL DEPOSITS UNDER VARIABLE CONDITIONS

Experimentally, three main types of stratal preservation have been recognised which arise from sudden variations in (1) the ratio between available sediment and sea level rise ( $V_s/SLR$ ), (2) the topography of the substrate, and (3) the morphological profile of the barrier ( $M$ ). All these types of preservation cause the drowning of the barrier, with local

preservation of its portions which, due to sea-level rise, are cut off from the active coastal zone (Sanders and Kumar, 1975; Belknap and Kraft, 1981; 1985). In our experiments the shoreface termination represents the boundary between this zone and the potential area of stratal preservation.

### Variations in the ratio of sediment supply to sea level rise

As the  $V_s/SLR$  ratio varies (Muto and Steel, 1997; 2000), preservation of coastal deposits may only be reproduced during two distinct phases, the first of which is characterised by high values of the above ratio and the second by markedly lower values. To these phases correspond respectively a period of barrier-growth and of barrier drowning with isolation of the preserved mass on the shelf. The simulations in Fig. 7 show this type of stratal preservation: the first four examples (A-D) involved successively assigning to the first phase (steps 0-15) and the second phase (steps 16-23) all possible combinations of conditions entailing stable or rising sea level (with different sand supply,  $V_s$ ). Thus, examples A (stable sea level for both first and second phases) and B (rising sea level for both) show barrier-drowning phenomena (preservation) due to variations in  $V_s$ . In comparison, case C (stable and rising sea level) involves the response to variations of SLR ( $V_s = \text{const.}$ ) while D (rising and stable sea level) involves responses to variations in SLR and  $V_s$ .

Figure 7A depicts evolution first with a sediment surplus (steps 0-15) and then with a deficit (16-23). The result is an initial progradation (steps 0-15) which includes the shelf ramp (c), the only deposit preserved in the course of the later erosional translations landwards (steps 16-23). The entire shoreface is depositional in the first phase (progradation) and erosive in the second (formation of ravinement surface). The horizontality of the ravinement surface is indicative of the stability of sea level during its formation.

The barrier drowning in Fig. 7B also derives from variations in  $V_s$ , but under conditions of a constant rate of sea-level rise throughout both phases. The sediment surplus (steps 0-15) causes retrogradational deposits on the top of the initial barrier from step zero (deposit a). Thus a thick littoral body is formed (step 15), which is markedly raised in comparison to coastal plain and therefore, under altered conditions, tends to give rise to rapid acceleration in barrier migration toward the mainland. This acceleration occurs due to the reduced sediment supply from step 16 ( $V_s=0$ ), and the barrier drowning is the product of the second transgressive phase. At the end of the evolution, the preserved shelf deposit includes the entire barrier from the start of the experiment (a), plus deposits (e) and (b).

Case in Fig. 7C reproduces the kinematics of "in place drowning", which is thought to occur typically when a period of stable sea level is followed by a rapid sea level rise (Sanders and Kumar, 1975; Boyd and Penland, 1984; Carter et al., 1986). The first phase is progradational and causes the development of a large barrier (see step 15) with a ramp (c), whilst the second phase, of drowning, is retrogradational and initially manifests itself as a rapid acceleration in barrier migration. At the end of the experiment the preserved deposit includes, apart from the initial sand body (a), prograding shoreface (d) and ramp (c) facies, plus back-barrier facies (b) in a transgressive arrangement (coastal onlap) which is the only facies formed during the second evolutionary phase.



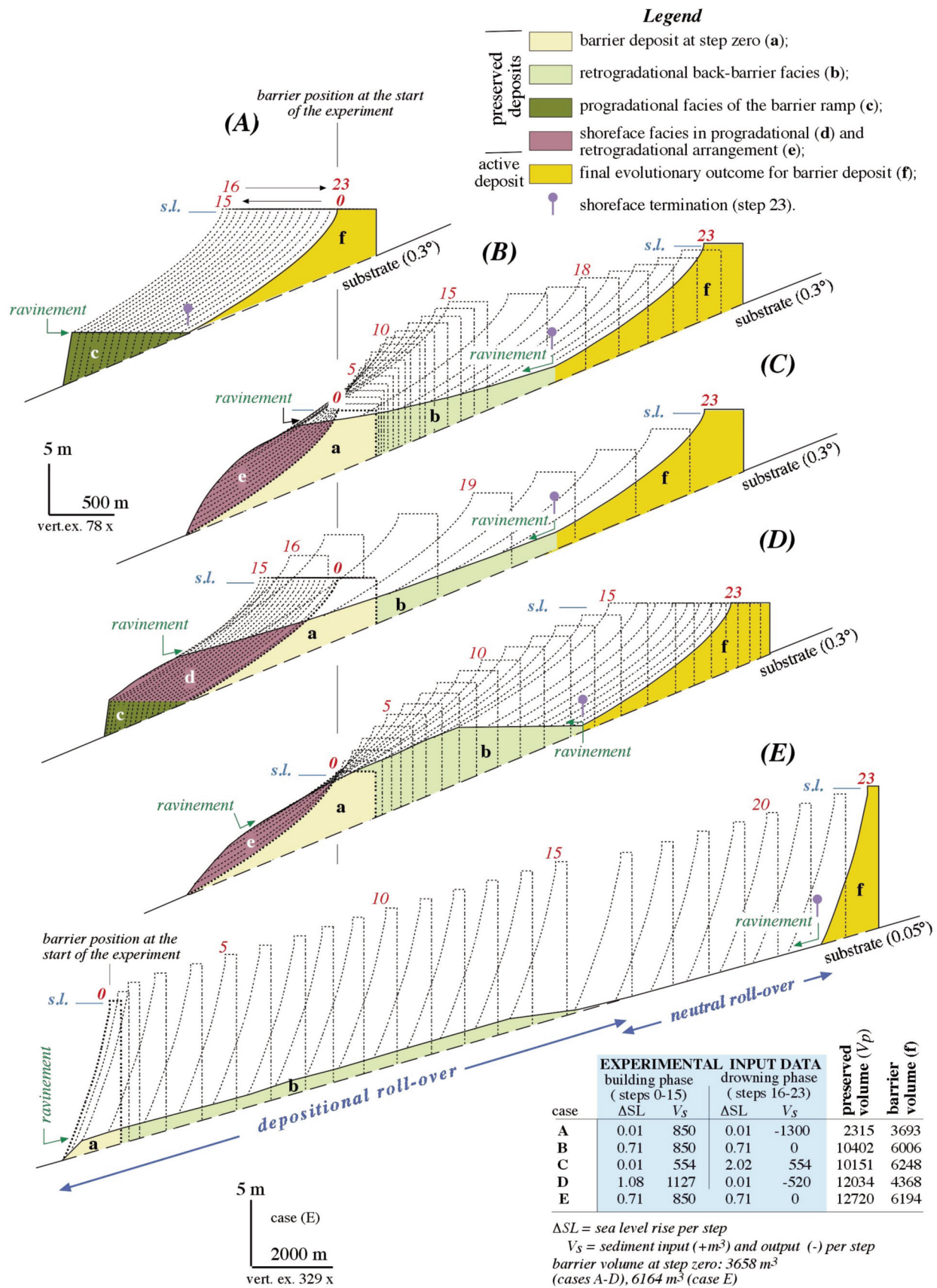


Fig. 7 - Examples of barrier drowning due to variation in the ratio of sediment supply to accommodation generation ( $V_s/SLR$ ) during two successive phases of evolution respectively dominated by high ratios (steps 0-15) and low ratios (steps 16-23): (A) conditions of stable sea level with +/- $V_s$  in successive periods; (B) variation in  $V_s$  only; (C) variation in SLR only; (D) variation in both  $V_s$  and SLR; (E) variation in  $V_s$  as the example B but over a lower substrate slope (0.05°). Inset table summarises input data used for the experiments.

In Fig. 7D, the first phase has significant sediment input that, however, does not compensate the constant rise in sea level. The result is a notable barrier translation accompanied by retrogradational deposits. The second phase, with stable sea level and high sediment export, causes progressive shoreface retreat with consequent formation of a "morphological terrace" (i.e. the ravinement surface). At the end of the evolution, the sand mass abandoned on the shelf includes the initial barrier (a), plus parts of the back-barrier (b) and shoreface facies (e). As in Fig. 7A, the ravinement surface formed during stable sea level is perfectly horizontal. Note that, as in other examples, the geometry of the preserved deposit is asymmetric, with the steepest side always facing seawards.

The examples discussed show that stratal preservation associated with conducive  $V_s$ /SLR can occur during either sea level rise and/or stability if the following conditions are fulfilled: (a) during the first phase,  $V_s$  almost fully or over compensates for the effects of rise in sea level; (b) during the second phase,  $V_s$  is much less than required to compensate for sea-level rise. The prerequisites for preservation are therefore values of the  $V_s$ /SLR ratio that first favour and then oppose growth and the stability of the barrier. The initial growth phase sequence is critical. For example, a barrier that does not grow by progradation ( $V_s \leq 0$ ) under conditions of stable sea level, will steadily migrate when sea level subsequently rises regardless of its rapidity or persistence. Under these circumstances the barrier will not be drowned to form a preserved sand mass.

In transgressions exhibiting low sediment input relative to the SLR, as in the case of several periods of the Late-Quaternary transgression, the first phase is generally critical with the preservation criteria outlined above having less bearing. Then, eustatic conditions favourable to stratal preservation are limited to those in Fig. 7C, which include an initial period of stable sea level. The sediment trapping effects of paleotopography (Belknap and Kraft, 1985), nevertheless, can create localised conditions conducive to preservation of the types shown in Fig. 7B and D) even during periods of rapid sea-level rise. For example, the field data analysed further below contain evidence of such trapping (Fig. 11C). Drowned barriers are preserved either side of a structural peak on the rocky seafloor. The peak formed an ancient promontory during the transgression, when the coast flanking it was initially well supplied due to the influence of the promontory on longshore drift (1<sup>st</sup> phase). Then, this segment of coast was starved of sediment (2<sup>nd</sup> phase) when the trapping effects of the promontory ceased as the sea level rose further (Tortora, 1996).

Shelf gradient plays a very important role in stratal preservation, such that the value of  $V_s$ /SLR ratio favouring drowning on certain gradients might not do so on others. This is supported by the case in Fig. 7E, in which simulated conditions were equivalent to those in Fig. 7B, except for a much lower gradient substrate (0.05° versus 0.3°). The low gradient is not conducive to drowning but gives rise to an extensive sand sheet (1<sup>st</sup> phase) and, subsequently, to the typical null effects of neutral roll-over (2<sup>nd</sup> phase). Barrier drowning is absent because  $V_s$  is too weak to provide sufficient compensation for the strong translational effects of SLR over the sub-horizontal shelf, thus suppressing the stalling in barrier translation essential for subsequent barrier drowning. The conclusion is that barrier-drowning is less favoured by lower shelf gradients.

### Variations in substrate topography

Figure 8 shows several cases in which a significant proportion of the barrier deposit is preserved exclusively due to morphological control of the substrate. Case A involves a neutral roll-over ( $V_s=0$ ) where, because the rapid increase in the shelf gradient (from 0.1° to 0.4°) raises the neutral point above the substrate, a portion of the barrier is no longer involved in neutral roll-over and is abandoned on the shelf. The result is a retrogradational deposit (b) bordered by the ravinement surface above. At the end of the process, the barrier volume (f) is drastically reduced, compared to step 0, by an amount equal to the total preserved mass (see table).

Case B (Fig. 8) develops on a shelf with a stronger increase in gradient (from 0.3° to 0.8°). Initially the evolution is very similar to A: the barrier proceeds in neutral roll-over and subsequently, where gradient varies, sheds a significant part of its volume as a preserved back-barrier deposit (b). During later evolution, the steeper portion of the substrate causes a change in the migration mode (from roll-over to encroachment: Tortora et al., 2009) with consequent seawards redeposition (e), above deposit (b), of sediments eroded from the substrate. The deposits (b) and (e) are separated by the ravinement surface, and in a strict sense only the former can be attributed to transgressive preservation (Belknap and Kraft, 1981; 1985). At the end of evolution the littoral sand body (f) has a notably lower volume than the initial one (step 0), contained entirely within the mid-lower shoreface region. The reduction in volume of the littoral body is equivalent to the difference between loss (the relict mass on the shelf: b and e) and gain (input from eroded substrate). This type of preserved deposit (b and e facies) has been identified in seismic records and modelled on the Columbia River shelf, NW USA (Stolper et al., 2005), off Montigue Island in SE Australia (Cowell et al., 1992), and on the Tyrrhenian shelf of Calabria, south Italy (Chiocci et al., 1989; Tortora et al., 2001).

Figure 8C refers to neutral roll-over migrating on a substrate with numerous morphological highs and lows. These irregularities are flattened out by the erosion of the highs and the infilling of the lows due to preservation of the coastal lithosome (deposit b). Modest seaward redeposition of the sediment previously eroded from the shoreface gives rise to the thin deposit (e) lying on the ravinement surface. The barrier at the end of the experiment (f) has a lower volume than at the beginning, with the losses due to preservation being greater than the gains from erosion of the substrate. Cowell et al. (1995) identify effects of stratal preservation within morphological lows in seismic and core data from SE Australia.

### Variation of the morphological barrier profile

Although unexplored in the literature, cases of preservation due to variations in the barrier profile were reproduced in simulation experiments. The examples in Fig. 9 show a barrier in neutral roll-over, in which certain of its morphological-profile parameters vary at step 4 (parameters  $h_w$ ,  $W_w$ ,  $L_w$ ,  $m$ ) producing stratal preservation due to: in case A, the raising of the neutral point at the toe of the shoreface (wave base,  $h_w$ ); in B, the reduction in width of the emerged barrier ( $W_w$ ); in C, the increased length of the shoreface ( $L_w$ ); in D, the increased concavity of the shoreface ( $m$ ). By imposing these same variations in pairs or all together (Table in Fig. 9), amplified effects on stratal preservation were obtained through the compound cases AB, CD, ABCD.

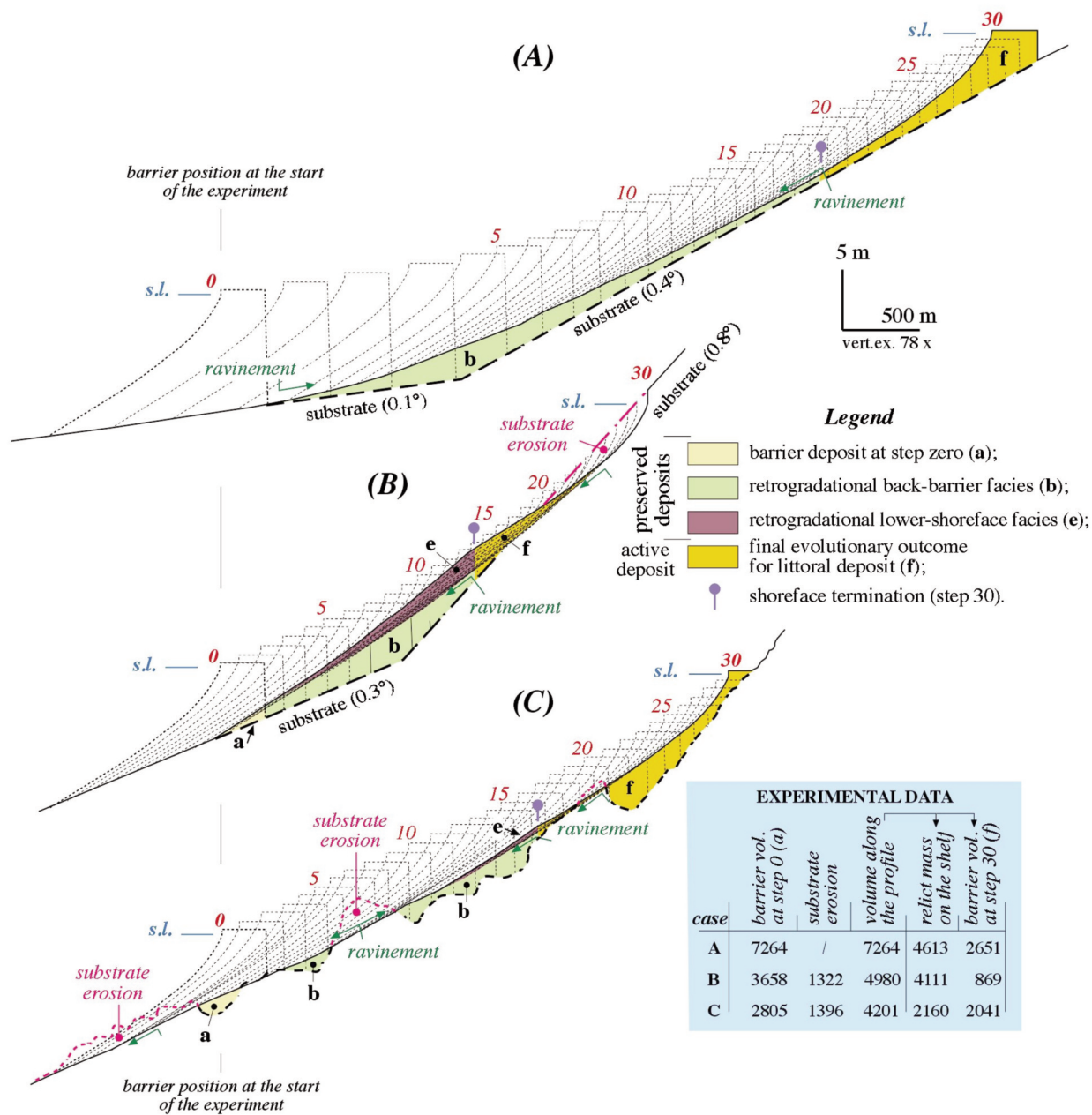


Fig. 8 - Stratigraphic preservation over irregular substrate topography: (A) preservation over a concave-upward substrate inflexion (deposit b); (B) preservation as in A but with additional deposit (e) formed during the later evolution over a steeper substrate, that is eroded with displacement of sediments to the lower shoreface; (C) transgressive smoothing of antecedent topography through erosion and fill respectively of peaks and depressions. The table gives simulated sediment-transfer volumes. Inputs per time-step:  $V_s=0$ ;  $SLR=0.71$  m.

The case AB (Fig. 9) is intended to simulate a coast rapidly affected by a decrease in wave energy, with consequent change in the wave base ( $h_w$ ) and loss of efficiency of the landwards sediment dispersal systems (washover, tidal flood delta) causing the width of the barrier ( $W_*$ ) to be reduced. Case CD shows possible effects due to reduced sediment size, manifest in the greater length of the shoreface ( $L_*$ ) and in a more pronounced concavity ( $m$ ) close to the shore (for the erosion due to the lack in coarse sediment). Case ABCD, which combines all the effects of the previous two examples, could represent a barrier migrating into a semi-protected coastal configuration influenced by a source of fine sediment. However, beyond these hypothetical environmental

references, all the cases of stratigraphic preservation (Fig. 9) imply rapid modifications of the barrier profile, possible only under strong paleo-topographic control. Therefore this type of preservation should occur on morphologically irregular shelves where, during transgression, changes in the shelf gradient and costal configuration can be expected to have consequences for the barrier profile.

### STRATIGRAPHIC ARRANGEMENT OF PRESERVED DEPOSITS

The stratigraphic arrangement of preserved deposits is a consequence of the migration path of the barrier, as shown in Fig. 10A for a depositional roll-over which evolves in



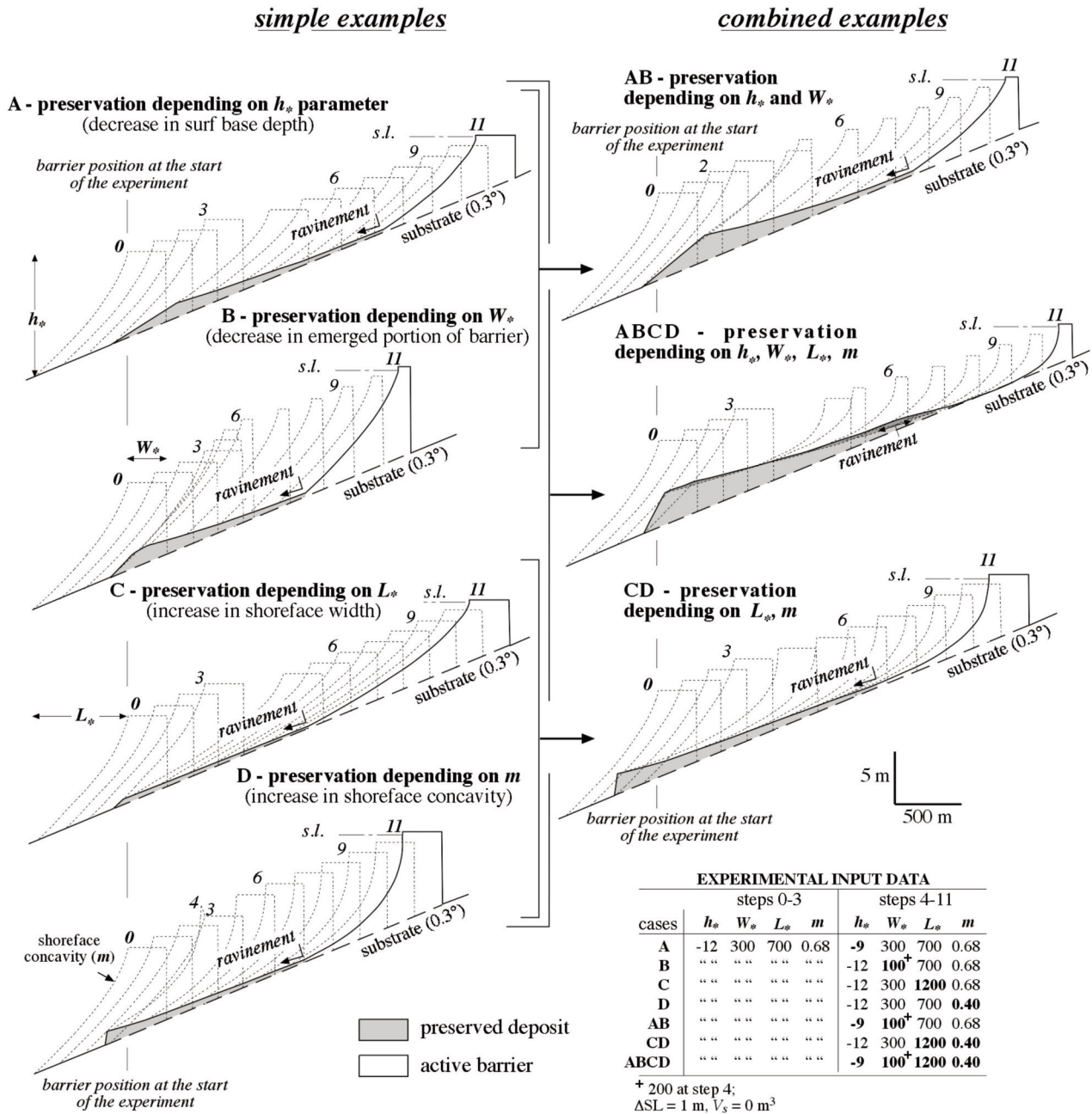


Fig. 9 - Stratigraphic preservation due to a rapid change (at time-step 4) in shoreface and barrier morphology involving variations in four geometric parameters: (A) maximum depth of the shoreface,  $h_*$ ; (B) subaerial barrier width,  $W_*$ ; (C) width of the shoreface,  $L_*$ ; (D) shoreface concavity,  $m$ ; (AB)  $h_*$  and  $W_*$ ; (CD)  $L_*$  and  $m$ ; (ABCD) all four parameters. Parameter values are listed in the table ( $V_s=0$  in all cases).

constant conditions ( $SLR$ ,  $V_s$ ,  $a$ ) and, therefore, with steady translations over time. The vector  $R_t$ , representing the resulting trajectory (steps 0-5), shows the successive positions of the crest of the berm with time. Any individual point along the barrier profile could trace the same trajectory but along a path of different elevation, provided the barrier profile does not vary through time. The vector  $R_t$  includes angle of trajectory ( $\theta$ ) and rate (vector length) of the stratigraphic growth (preceding passage of the shoreface). This vector, for a given point of the barrier profile, therefore represents the continual repetition of a single facies (the berm in the case of the Fig. 10) which, within a stratigraphic section, is used to define the depositional arrangement

(progradational, aggradational or retrogradational). For evolutions under variable conditions, successive  $R_t$  vectors form a broken line in representing the trajectory variations during barrier migration. The factors controlling this trajectory ( $SLR$ ,  $V_s$ ,  $a$ ) therefore also control the stratigraphic arrangement of preserved deposits, which can also be modified by the effects of possible changes in the morphology of the barrier profile ( $M$ ).

Two depositional domains (Fig. 10B) can be inferred from the above principles (Curry, 1964; Helland-Hansen and Martinsen, 1996; Cattaneo and Steel, 2003) under the limiting conditions of only stable or rising sea level ( $\Delta SL \geq 0$ ). In the diagram the vector  $R_t$  represents a hypothetical

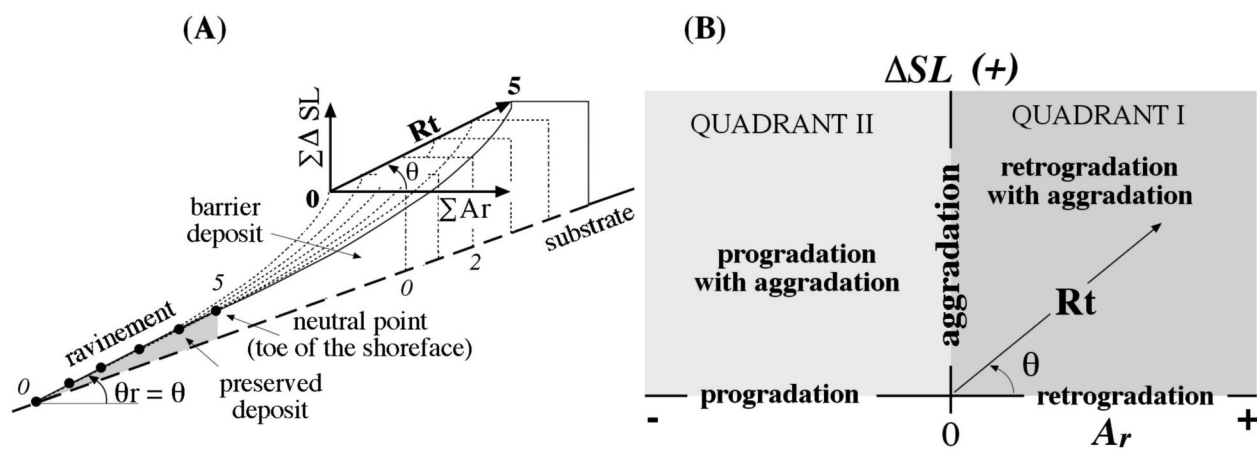


Fig. 10 - Shoreface-translation trajectory (vector  $R_t$ ) and stratal preservation. In A, example of a coastal system evolving under constant conditions of positive supply and sea-level rise. In B, phase diagram for stable and rising sea-level (y-axis) and shoreline translation (x-axis). Quadrants of the preservation phase diagram signify: (1) pure retrogradation ( $A_r > 0$ ;  $\theta = 0$ ); (2) retrogradation with aggradation (backstepping deposits:  $A_r > 0$ ;  $0 < \theta < 90^\circ$ ); (3) pure aggradation ( $A_r = 0$ ;  $\theta = 90^\circ$ ); (4) progradation with aggradation ( $A_r < 0$ ;  $90 < \theta < 180^\circ$ ); (5) pure progradation ( $A_r < 0$ ;  $\theta = 180^\circ$ ).

landwards translation,  $A_r > 0$  ( $A_r < 0$  for seawards translations). Theoretically, this vector rotates ( $\theta$  varies) and changes in magnitude as a function of sediment supply for a given SLR (the ratio  $V_s/\text{SLR}$ ). Thus, for a pre-established barrier morphology ( $M$ ) and substrate gradient ( $a$ ), only one  $R_t$  value is possible for a given value of  $V_s/\text{SLR}$  in producing pure aggradation ( $\theta = 90^\circ$ ), when  $V_s$  perfectly offsets the effects of SLR. An increase or decrease in the  $V_s/\text{SLR}$  ratio about the threshold of balance, shifts  $R_t$  respectively into Quadrant II (progradation with aggradation:  $90 < \theta < 180^\circ$ ) or Quadrant I (retrogradation with aggradation:  $0 < \theta < 90^\circ$  positive). Pure progradational and retrogradational effects, on the other hand, occur when  $\text{SLR} = 0$  and  $V_s$  is positive ( $\theta = 180^\circ$ ) or negative ( $\theta = 0^\circ$ ) respectively.

## EVOLUTIONARY RECONSTRUCTION APPLIED TO A REAL CASE

### The area under examination

Figure 11 shows the characteristics of the Late-Quaternary shelf deposits, near Argentario promontory (Tuscan region, Italy), whose dynamics of formation have been reconstructed along the section A-B using the STM. From the available data (Tortora, 1996), the existing transgressive unit (transgressive systems tract: TST) overlies the unconformity created during the preceding sub-aerial exposure of the shelf. This surface contains irregularities in the middle part of the section, particularly where a limestone substrate crops out giving rise to a small island (Formiche di Burano) surrounded by rocky seafloor (Fig. 11A). The thickness of the TST (Fig. 11B) is greatest either side of the outcrop (5-7 m), remains significant (3-5 m) on the intermediate water depths, and is thinner further offshore (1.5-3 m) and closer to the coast (0-1.5 m). The TST is composed of three vertical successions of facies (A, B, C) distributed throughout the area (Fig. 11C). Their stratigraphic columns comprise (from bottom to top): for column A, lagoonal strata, washover and lower shoreface deposits, the latter above the ravinement surface (Fig. 12A, record 2); for column B, lower-shoreface sediments (Fig. 12A, record 1); and for column C, a very reduced generally basal lag deposit. Two further sedimentary bodies, with prograding internal reflectors, are

present on either side of the limestone outcrop (Fig. 11C). They are attributable to an episode of barrier drowning occurred during the sea level rise (as in Fig. 7B).

### Simulation Techniques

The STM reconstruction draws from the available geological data and is validated at each time interval by the correlation between real and simulated evidence: i.e., the inverse method (Tarantola, 1987). For the shelf section under investigation, the control data consist of a high-resolution seismic line (coinciding with the section) and related gravity-core calibrations; the characteristics of the transgressive unit in the surrounding area also provide orientation (Aiello et al., 1978; Tortora, 1996). For the coastal part of the section, the control data are only superficial (sedimentological and topobathymetric) and the simulation is mostly a prediction of the modern barrier stratigraphy. Contributing to the reliability of this prediction is the reconstruction of the last transgressive phase, the trend in which was used to guide the geological forecast during successive periods.

Input data to reconstruct the evolution of the field area included the topography of the unconformity surface (digitized from the seismic record), assumed to define the plane over which the transgression occurred. For the littoral part of the section, this topography was extrapolated from shallow seismic data. The simulation is divided into time steps of 300 years duration. The rate of SLR for each step was derived from the eustatic curve in Bellotti et al. (1995). Rates of sediment input on the coast ( $V_s$ ) and on the lagoon behind it ( $V_m$ ) were obtained through repeated calibrations (for each step) to optimise the rates needed to regenerate the measured stratigraphic features (i.e. the inverse method). Parameter estimates for barrier-profile morphology were based on topographic and sedimentological data taken from the modern littoral barrier, the latter used to evaluate the length and maximum depth of the shoreface ( $L_s, h_s$ ) from the transition between sand and mud (i.e. the mud-line). The presence of lower-shoreface facies (Fig. 11C), linked to modest seaward reworking of sediments during the transgression, indicated the use of a concave shoreface profile (specifically,  $m \leq 0.2$ ). Results for each time step were validated by the comparison of measured and STM modelled

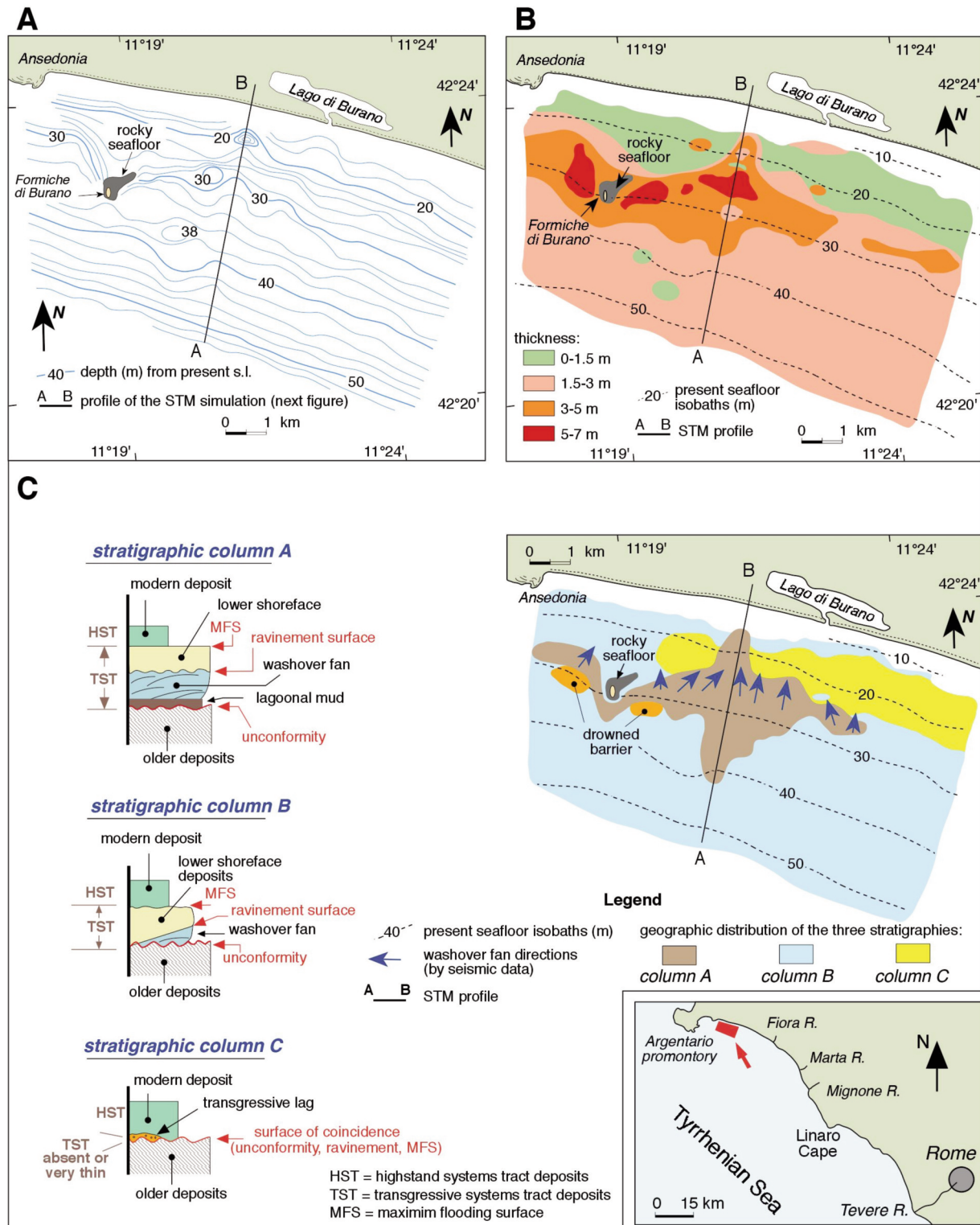


Fig. 11 - Transgressive deposit, mapped from field data, whose evolution was simulated along section A-B (Fig. 12): (A) contour map of the lowstand unconformity (meters relative to present sea level) corresponding to the land-surface over which transgression occurred; (B) isobath map of TST deposit (in meters); (C) sedimentary facies columns and their geographic distribution.

data (tracking parameters). Visual comparisons were also checked through superposition of STM output plots over the data model with the real shelf stratigraphy. This data model, deriving from seismic and coring records, has included the topography of relevant surfaces (unconformity, ravinement, maximum flooding, present bathymetry and sub-aerial

morphology) and references related to the geographic limits of the TST facies sequences along the section (Fig. 11C).

Values of the input and tracking parameters are given in Table 1. The simulation was commenced at the edge of the continental shelf (parameters from Aiello et al., 1978) to ensure full windup of the kinematics before translation of



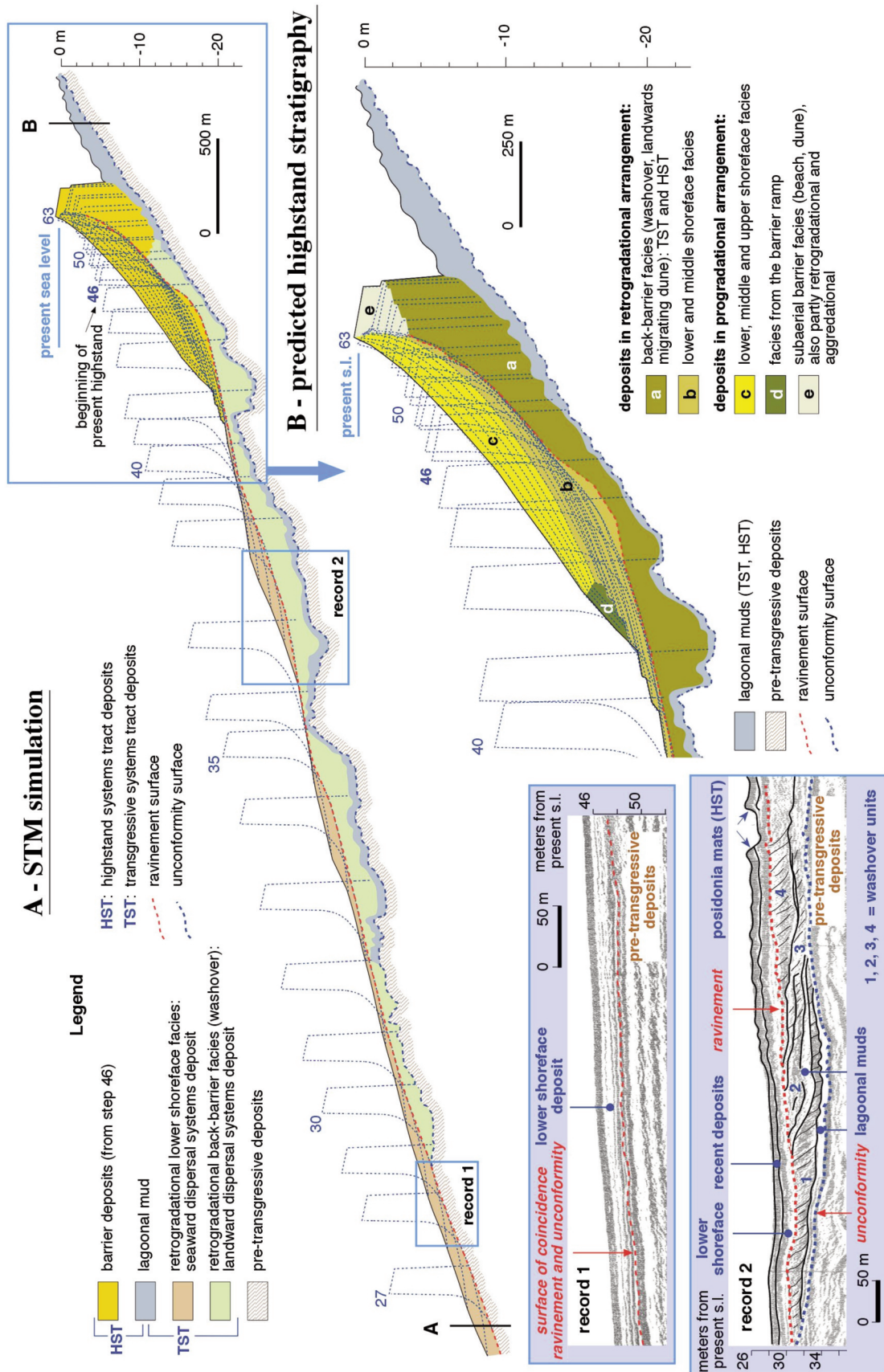


Fig. 12 - Simulated evolution of TST shown in Fig. 11 (section A-B) modelled using interactive inversion methods: (A) transgressive phase (time-steps 27-46) with simulation output overlaid on stratigraphy reconstructed from field evidence for comparison; (B) highstand phase (from time-step 46) with the predicted barrier stratigraphy.

time steps	age (years) from present	sea level (m) with respect to present	sea level rise per step (m)	morphological parameters of barrier profile				depositional rate (m) of lagoonal mud ( $V_m$ )	sand input ( $m^3$ ) to the barrier ( $V_s$ )	sedimentary dynamics				geometric elements					
				$L_*$	$h_*$	$m$	$W_*$			barrier erosion ( $m^3$ ) by shoreface translation (cut)	sand transported landwards ( $m^3$ ) and redeposited on the back-barrier (internal fill)	sand transported seawards ( $m^3$ ) and redeposited on the shoreface (ext. fill)	total sand ( $m^3$ ) deposited (int. and ext. fill)	thickness (m) of preserved deposit (S): between unconformity and ravinement surface (n. point)	horizontal translations ( $A_r$ ) in m (negative values are seawards translations)	angle ( $\theta$ ) of barrier migration trajectory	water depth (m) of the neutral point	distance (m) from the shoreline of the neutral point	
27	-10800	-50.19		730	16	0.15	150												
28	-10500	-42.54	3.5	"	"	"	"	0.00	700	1574	1577	696	2274	0.0	383	0.52	13.4	219	
29	-10200	-39.03	2.5	"	"	"	"	0.00	900	1546	1855	590	2446	0.4	252	0.57	13.1	197	
30	-9900	-36.52	2.5	"	"	"	"	0.00	1000	1650	2223	427	2650	1.7	315	0.46	13.7	256	
31	-9600	-34.00	2.5	"	"	"	"	0.00	1000	1570	2046	523	2570	2.2	275	0.52	13.4	219	
32	-9300	-31.49	2.7	"	"	"	"	0.72	1000	1718	2360	358	2718	1.3	375	0.41	13.9	292	
33	-9000	-28.81	2.7	"	"	"	"	0.72	1000	1798	2530	268	2798	1.5	420	0.37	14.2	334	
34	-8700	-26.13	2.5	"	"	"	"	0.00	1000	1845	2668	176	2845	4.2	442	0.33	14.5	382	
35	-8400	-23.61	2.2	"	"	"	"	0.00	1000	1793	2581	211	2793	3.1	352	0.35	14.3	347	
36	-8100	-21.43	2.2	"	"	"	"	0.48	1000	1468	1887	580	2468	3.0	198	0.63	12.9	175	
37	-7800	-19.25	2.2	"	"	"	"	0.48	1000	1867	2689	177	2867	1.4	375	0.33	14.5	371	
38	-7500	-17.06	2.2	"	"	"	"	0.00	800	2174	2962	12	2974	4.4	540	0.23	15.4	572	
39	-7200	-14.88	1.7	"	"	"	"	0.00	800	1613	2132	280	2413	4.2	219	0.44	13.8	267	
40	-6900	-13.19	1.7	"	"	"	"	0.00	800	1475	1872	402	2275	3.7	171	0.56	13.2	201	
41	-6600	-11.50	1.5	"	"	"	"	0.00	800	1351	1742	408	2151	3.2	139	0.63	12.9	177	
42	-6300	-9.98	1.2	"	"	"	"	0.00	800	1440	2002	237	2240	3.0	139	0.49	13.5	237	
43	-6000	-8.79	1.0	"	"	"	"	0.00	600	2086	2684	1	2686	2.6	285	0.21	15.7	653	
44	-5700	-7.76	1.0	"	"	"	"	0.00	400	1712	2023	88	2112	4.8	178	0.33	14.5	380	
45	-5400	-6.74	0.7	"	"	"	"	0.00	200	1335	1450	85	1535	2.8	116	0.36	14.3	338	
46	-5100	-6.00	0.6	"	"	0.20	"	0.03	200	1291	1428	62	1491	4.5	135	0.25	15.3	534	
47	-4800	-5.42	0.4	"	"	"	"	0.04	200	238	297	140	438	1.5	26	0.95	12.0	107	
48	-4500	-4.98	0.4	"	"	0.25	"	0.04	200	532	632	99	732	5.5	68	0.29	16.0	730	
49	-4200	-4.63	0.3	"	"	"	"	0.05	200	83	145	137	283	4.1	12	1.57	8.7	95	
50	-3900	-4.29	0.3	"	"	0.30	"	0.05	200	400	520	80	600	5.7	59	0.33	16.0	730	
51	-3600	-3.95	0.5	"	"	"	"	0.08	200	163	247	116	363	3.0	23	1.08	10.2	162	
52	-3300	-3.50	0.5	"	"	0.35	"	0.08	200	404	547	57	604	3.6	65	0.40	15.5	658	
53	-3000	-3.04	0.4	"	"	"	"	0.07	200	116	205	111	316	2.5	20	1.21	9.7	137	
54	-2700	-2.61	0.3	"	"	0.40	"	0.04	200	222	350	72	422	4.1	44	0.42	16.0	730	
55	-2400	-2.28	0.4	"	"	"	"	0.05	200	47	130	116	247	5.1	11	1.70	7.1	95	
56	-2100	-1.93	0.3	"	"	0.45	"	0.04	200	165	290	74	365	4.7	39	0.48	16.0	730	
57	-1800	-1.60	0.3	"	"	0.48	"	0.04	300	27	114	212	327	5.6	12	1.39	7.2	150	
58	-1500	-1.29	0.3	"	"	0.50	"	0.00	400	0	0	400	400	5.4	-4	-3.73	16.0	730	
59	-1200	-0.99	0.3	"	"	0.53	"	0.03	500	0	3	496	500	5.7	-5	-2.72	16.0	730	
60	-900	-0.71	0.2	"	"	0.56	"	0.01	500	0	0	499	500	5.6	-11	-0.90	16.0	730	
61	-600	-0.53	0.2	"	"	0.59	"	0.00	500	0	0	499	500	5.3	-10	-0.89	16.0	730	
62	-300	-0.36	0.2	"	"	0.63	"	0.03	500	0	0	499	500	5.5	-9	-1.05	16.0	730	
63	0	-0.19	0.2	"	"	0.75	"	0.11	500	23	170	352	523	6.0	18	0.59	16.0	730	

Tab. 1 - Input and output data for the simulation shown in Fig. 12.

the coastal system into the study section, although the STM evolution in the windup region (mid-outer shelf) is not shown in Fig. 12.

### Evolutionary reconstruction

The STM simulation (Fig. 12) dates the initial translation of the coastal barrier into the study section to approximately 10,800 years ago (step 27). Once the barrier had migrated across the inner shelf, its rate of retreat progressively diminished until the coast began to stabilise about 5,100 years ago (step 46), at the beginning of the highstand which continued through to the present (step 63). In the transgressive and highstand simulated-periods the total coastline retreat ( $A_r$ , horizontal translation) was respectively 5,179 m and 496 m, giving an average annual rate of around 1m and 0.1m.

During the first period (transgression), barrier migration (Fig. 12A) occurs through the hybrid mode of translation, toward the roll-over end of the continuum (Tortora et al., 2009). This simulated behaviour causes material eroded from the upper and middle shoreface erosion (cut) to be displaced landwards and, to a lesser extent, seawards (Fig. 13G). The result is a barrier that is progressively regenerated in a more

landward position, supplied from its own reworked material (cut) augmented by an external sediment supply ( $V_s$ ). Both cut and supply volumes are transferred and deposited (fill) at the margins of the eroded zone: on the sub-aerial coast (beach and back-barrier), through washover processes, and on the lower shoreface through shoreface retreat mechanisms (Sanders and Kumar, 1975).

The amount of transported sediment (Fig. 13G) indicates a barrier regeneration process that is initially very active but then sharply declines (from step 42), when the migration velocity decreases (the transport and translation data are correlated:  $r = 0.92$ ). The barrier migration is accompanied by deposits left progressively on the shelf, distinctly showing two stratigraphic units, bound by the ravinement surface wherever both are present (Fig. 12A, record 2). The lower unit (washover and lagoonal mud deposits) consists of the portion of the barrier preserved during the passage of the transgression. The upper unit includes the sediments redeposited on the lower shoreface (Fig. 12A, record 1), between original water depths of 12 and 16 m (between the neutral point and the offshore limit of the shoreface, Tab. 1). Stratal preservation is strongly controlled by the irregularities of the substrate and is greatest within the



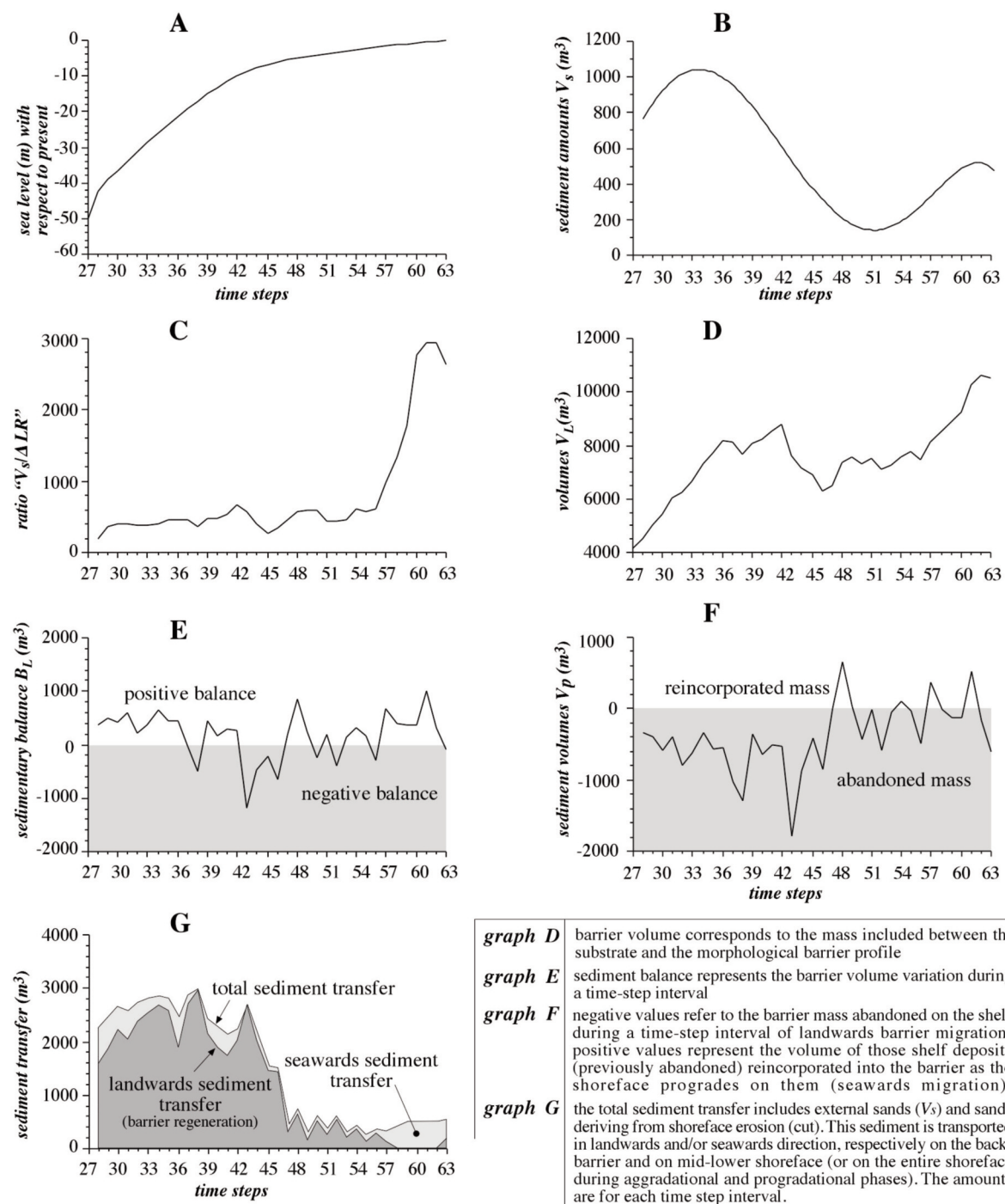


Fig. 13 - Variations through time (300 yr time step) of governing variables and tracking parameters for simulation in Fig. 12: (A) sea level relative to present; (B) littoral sand supply ( $V_s$ ); (C) degree of compensation by sand supply for effects of sea-level rise ( $V_s/DSL$ ); (D) barrier volume; (E) sediment balance (barrier-volume change); (F) sediment mass abandoned on the shelf (negative volumes) or reincorporated into the barrier (positive volumes); (G) cross-shoreface sand transfers during transgression.

depressions (similar to the case in Fig. 8C). The lower unit, lying on the unconformity, represents the back-barrier sedimentary mass not involved in the transgressive erosion, and then preserved. Its upper boundary, the ravinement surface, corresponds to the true plane of translation on which the barrier has migrated (Tortora et al., 2009, Fig. 4) and to the neutral point trajectory.

The transgression (steps 27-46) occurs under variable conditions (Fig. 13A, B and C) and consequently through kinematics which involve kinematic inertia (Tortora et al.,

2009), indirectly recorded by the strong instability of the sedimentary balance (13E). From the simulation data, the rate of sediment input per unit of SLR ( $V_s/SLR$ , Fig. 13C) is the main factor controlling the products of transgression. This rate is partially correlated with barrier volumes in Fig. 13D ( $r=0.86$ ; 5<sup>th</sup> order polynomial) and with amounts of stratal preservation in Fig. 13F ( $r=0.72$ , 5<sup>th</sup> order polynomial), as normally expected during a depositional roll-over (see Figs 3 and 5). The partial correlations mostly reflect the influence of the irregular paleotopography, especially the depressions



which amplify stratal preservation with consequent decreased barrier volume due to the sediment sequestered by the depressions (Fig. 8C).

Changes in the sediment balance (Fig. 13E) aggregate the effects of variations through time in all those parameters that contribute to the balance during the transgression (Tortora et al., 2009). These parameters are: (1) the ratio of external sediment-supply to accommodation space (Fig. 13C, correlated with balance:  $r=0.70$ , 5<sup>th</sup> order pol.); (2) the sediment lost on the shelf as stratal preservation (Fig. 13F,  $r=0.86$ , 5<sup>th</sup> order pol.); and (3) sediment reworked seawards (Fig. 13G,  $r=0.92$ , 5<sup>th</sup> order pol.) which is often related to translation of the barrier over morphological highs (hybrid migration). Although the coast is continually supplied with sediment ( $V_s$ ), periods of negative imbalance occur when stratal preservation (in depressions) exceeds supply. The sediment availability ( $V_s$ ) reflects the influences external to the section. Specifically the ancient promontory that lies a little to the west from the section (Fig. 11A, Formiche di Burano), is likely to have trapped sand from the longshore drift when the sea was about 18 to 30 m below its present level. Similar effects, on a more regional scale, were probably caused by the larger promontory of Monte Argentario, located several kilometres west from the section (Fig. 11).

The simulated highstand stratigraphy of the barrier (Fig. 12B) comprise five facies: retrograding back-barrier (a) and mid-lower shoreface (b) facies; more recent deposits (c, d, e) mostly in a progradational setting; and the lagoonal mud at the base of the sequence. The conditions which distinguish the highstand from the transgressive phase are strongly evident in the diagram of Fig. 13C.

## CONCLUSION

During periods of sea level rise, coastal preservation comprises those parts of the barrier, below the maximum depth of shoreface erosion (i.e. the neutral point depth), which do not migrate landwards. The resulting deposits abandoned on the shelf are bound from above by the ravinement surface and from below by the substrate, that is the paleotopography (unconformity) on which the transgression occurs. The degree of stratal preservation corresponds to the vertical distance between these two surfaces. Kinematics and stratal preservation are governed by (1) sea level rise, (2) littoral sediment supply ( $V_s$ ), (3) substrate gradient ( $\alpha$ ), and (4) the morphological profile of the barrier ( $M$ ).

Stratal preservation can occur under various conditions defined by the drivers listed above (SLR,  $V_s$ ,  $\alpha$ , and  $M$ ). During transgressive phases with relatively constant conditions, preservation only occurs in conjunction with positive sediment supply ( $V_s > 0$ ). The resulting deposits are distinguishable by their geometry and internal facies. With increased SLR, decreased  $+V_s$  and lowered  $\alpha$ , the geometry is increasingly tabular. As  $V_s/\text{SLR} \rightarrow 0$  or  $\alpha \rightarrow 0$ , the facies are reduced to those of the basal stratigraphy that existed before the passing of the transgression. Methods have been proposed for (a) predicting the geometry of these deposits for given values of SLR,  $V_s$  and  $\alpha$ , (b) defining their age of formation and that of the ravinement surface lying above them, and (c) locating the position of the coastline respectively associated to these two ages.

During transgressive phases subject to highly variable environmental conditions ( $V_s/\text{SLR}$ ,  $\alpha$ , and  $M$ ), especially

when these occur as rapid perturbations, preservation occurs as three types of adaptive morpho-kinematic responses. The first type of stratal preservation requires two distinct periods of evolution, successively involving high and low values of the ratio  $V_s/\text{SLR}$ . To these periods correspond barrier growth followed by barrier drowning when sudden landward displacement occurs. This type of preservation can eventuate under a variety of eustatic contexts and, thus, its occurrence is probably the most common in nature. Nonetheless, in rapid transgressions, such as those on sub-horizontal shelves and/or with sediment input well below that required to compensate the SLR (such as during the Holocene transgression), this type of preservation requires an initial period of near stable sea level. Such stability is necessary to condition the barrier, through its growth, for susceptibility to drowning during the subsequent phase. For all cases examined in which preservation was attributable to  $V_s/\text{SLR}$ , the preserved deposit was asymmetric with the steepest side always facing seawards and with a terrace at its upper surface (i.e. the ravinement). Terrace slope gently up to landwards, such that the height difference between each end corresponds to the sea-level rise during the barrier-drowning event.

The second type of stratal preservation occurs on morphologically irregular shelves. More specifically, it is favoured at the base of abruptly increased steepness, or within morphological depressions. The third type derives from rapid changes of the barrier profile, such as a reduction in barrier width or geometry of the shoreface (its surf-base depth, width or concavity). These changes are more likely on irregular shelves where, during transgression, variations in the antecedent topography have rapid repercussions on the barrier profile.

Whatever the cause of stratal preservation, the stratigraphic setting of resulting deposits depends on the trajectory of the barrier migration and, more fundamentally, on the factors which control it (SLR,  $V_s$ ,  $\alpha$ ,  $M$ ). The reconstruction of the Holocene evolution along a section of Tuscan shelf-coast, suggests that, in nature, stratal preservation is often the result of multiple causes: in the specific case, the irregular paleotopography and the variations over time in  $V_s/\text{SLR}$  ratio. More generally, correct identification of the possible causes is difficult to ascertain because the drivers (SLR,  $V_s$ ,  $\alpha$ ,  $M$ ) of coastal preservation work strictly in conjunction. In any case, the diagnosis requires a three dimensional geological framework since occurrences along a shelf section are often dependent on what happens in adjacent areas. In the Tuscan shelf section, the external influence is exerted through variations in size of the coastal compartment during transgression, which in turn have governed the sediment inputs and their effects on potential preservation.

**ACKNOWLEDGMENTS** - This study is the result of a scientific collaboration between the Department of Earth Science of University "La Sapienza" of Rome and the Institute of Marine Science, School of Geosciences, of Sydney University. Financial support was provided by various Italian and Australia grants. The authors want to thank S. Milli, B. Murray and P. Roy for their stimulating comments on the manuscript.

## REFERENCES

- Aiello E., Bartolini C., Gabbanì G., Rossi S., Valeri G., Certini I., Clerici C., Lenaz R. 1978. Studio della piattaforma continentale medio tirrenica per la ricerca di sabbie metallifere: 1) da Capo Linaro a Monte Argentario. *Bollettino della Società Geologica Italiana*: 97, 495-525.
- Belknap D.F., Kraft J.G. 1981. Preservation potential of transgressive coastal lithosomes on the U.S. Atlantic shelf. *Marine Geology*: 42, 429-442.
- Belknap D.F., Kraft J.G. 1985. Influence of antecedent geology on stratigraphic preservation potential and evolution of Delaware's barrier systems. In: Oertel, G.F., Leatherman, S.P. (Eds.), *Barrier islands*. *Marine Geology*: 63, 235-262.
- Bellotti P., Milli S., Tortora P., Valeri P. 1995. Physical stratigraphy and sedimentology of the Late Pleistocene-Holocene Tiber Delta depositional sequence. *Sedimentology*: 42, 617-634.
- Boyd R., Penland S. 1984. Shoreface translation and the Holocene stratigraphy record: examples from Nova Scotia, the Mississippi delta, and Eastern Australia. *Marine Geology*: 60, 391-412.
- Carter R.M., Carter L., Johnson D.P. 1986. Submerged shorelines in the SW Pacific: evidence for an episodic post-glacial transgression. *Sedimentology*: 33, 629-649.
- Cattaneo A., Steel R.J. 2003. Transgressive deposits: a review of their variability. *Earth-Science Reviews*: 62, 187-228.
- Chiocci F.L., D'Angelo S., Orlando L., Pantaleone A. 1989. Evolution of the Holocene shelf sedimentation defined by high-resolution seismic stratigraphy and sequence analysis (Calabro-Tyrrhenian continental shelf). *Memorie della Società Geologica Italiana*: 48, 359-380.
- Cowell P.J., Roy P.S. 1988. *Shoreface Transgression Model: Programming Guide (Outline, Assumptions and Methodology)*. Unpub Report, Coastal Studies Unit, Marine Studies Centre, University of Sydney, 23pp.
- Cowell P.J., Roy P.S., Cleveringa J., De Boer P.L. 1999. Simulating coastal systems tracts using the shoreface translation model. *SEPM (Society for Sedimentary Geology), Special Publication*: 41, 165-175.
- Cowell P.J., Roy P.S., Jones R.A. 1992. Shoreface Translation Model: computer simulation of coastal-sand-body response to sea level rise. *Mathematics and Computers in Simulation*: 33, 603-608.
- Cowell P.J., Roy P.S., Jones R.A. 1995. Simulation of large-scale coastal change using a morphological behaviour model. *Marine Geology*: 126, 45-61.
- Cowell P.J., Stive M.J.F., Niedoroda A.W., De Vriend D.J., Swift D.J.P., Kaminsky G.M., Capobianco M. 2003a. The Coastal-Tract (Part 1): A conceptual approach to aggregated modelling of low-order coastal change. *Journal of Coastal Research*: 19, 812-827.
- Cowell P.J., Stive M.J.F., Niedoroda A.W., Swift D.J.P., De Vriend D.J., Buijsman M.C., Nicholls R.J., Roy P.S., Kaminsky G.M., Cleveringa J., Reed C.W., De Boer P.L. 2003b. The Coastal-Tract (Part 2): Applications of aggregated modeling to low-order coastal change. *Journal of Coastal Research*: 19, 828-848.
- Cowell P.J., Thom B.G. 1994. Morphodynamics of coastal evolution. In: Carter R.W.G., Woodroffe C.D. (Eds.), *Coastal Evolution: Late Quaternary Shoreline Morphodynamics*, Cambridge University Press, Cambridge, 33-86.
- Curry J.R. 1964. Transgressions and regressions. In: Miller R.L. (Ed.), *Papers in Marine Geology*. Macmillan, New York, 175-203.
- Dean R.G. 1991. Equilibrium beach profile: characteristics and applications. *Journal of Coastal Research*: 7, 53-84.
- Dean R.G., Maurmeyer E.M. 1983. Model of beach profile responses. In: Komar P.D., Moore J. (Eds.), *Handbook of Coastal Processes and Erosion*. Boca Raton, CRC Press: 151-165.
- Dillenburg S.R., Roy P.S., Cowell P.J., Tonazelli L. 2000. Influence of antecedent topography on coastal evolution as tested by the Shoreface Translation Barrier Model (STM). *Journal of Coastal Research*: 16, 71-81.
- Helland-Hansen W., Martinsen O.J. 1996. Shoreline trajectories and sequences: description of variable depositional-dip scenarios. *Journal of Sedimentary Research*: 66, 670-688.
- Heward A.P. 1981. A review of wave-dominated clastic shoreline deposits. *Earth-Science Reviews*: 17, 223-276.
- Kench P.S., Cowell P.J. 2001. The morphological response of atoll islands to sea-level rise. Part 2: Application of the modified shoreline translation model (STM). *Journal of Coastal Research*: 34, 645-656.
- Leatherman S.P. 1983. Barrier dynamics and landward migration with Holocene sea-level rise. *Nature*: 301, 415-418.
- Muto T., Steel R.J. 1997. Principles of regression and transgression: the nature of the interplay between accommodation and sedimentary supply. *Journal of Sedimentary Research*: 67, 994-1000.
- Muto T., Steel R.J. 2000. The accommodation concept in sequence stratigraphy; some dimensional problems and possible redefinitions. *Sedimentary Geology*: 130, 1-10.
- Niedoroda A.W., Reed C.W., Swift D.J.P. 1995. Modelling shore-normal large-scale coastal evolution. *Marine Geology*: 126, 181-199.
- Roy P.S., Cowell P.J., Ferland M.A., Thom B.G. 1994. Wave dominated coasts. In: Carter R.W.G., Woodroffe C.D. (Eds.), *Coastal evolution: late Quaternary shoreline morphodynamics*. Cambridge University Press, Cambridge, 121-186.
- Sanders J.E., Kumar N. 1975. Evidence of shoreface retreat and in-place "drowning" during Holocene submergence of barriers, shelf off of Fire Island, New York. *Geological Society of America Bulletin*: 86, 65-76.
- Stive M.J.F., De Vriend H.J. 1995. Modelling shoreface profile evolution. *Marine Geology*: 124, 235-248.
- Stolper D., List J.H., Thieler R.E. 2005. Simulating the evolution of coastal morphology and stratigraphy with a new morphological-behaviour model (GEOMBEST). *Marine Geology*: 218, 17-36.
- Swift D.J.P., Phillips S., Thorne J.A. 1991. Sedimentation on continental margin, IV: lithofacies and depositional systems. In: Swift D.J.P., Oertel G.F., Tillman R.W., Thorne J.A. (Eds.), *Shelf sand and sandstone bodies, geometry, facies and sequence stratigraphy*. International Association of Sedimentologists, Special Publication: 14, 89-152, Blackwell Scientific Publications.
- Tarantola A. 1987. Inverse problem theory: methods for data fitting and model parameter estimations. Elsevier, Amsterdam, 613 pp.
- Thorne J.A., Swift D.J.P. 1991. Sedimentation on continental margins: VI. A regime model for depositional sequences, their component systems tracts, and bounding surfaces. In: Swift D.J.P., Oertel G.F., Tillman R.W., Thorne J.A. (Eds.), *Shelf Sand and Sandstone Bodies, Geometry, Facies and Sequence Stratigraphy*. International Association of Sedimentologists, Special Publication: 14, 189-255, Blackwell Scientific Publications.
- Tortora P. 1996. Depositional and erosional coastal processes during the last postglacial sea-level rise: an example from the central Tyrrhenian continental shelf (Italy). *Journal of Sedimentary Research*: 66, 391-405.
- Tortora P., Bellotti P., Valeri P. 2001. Late-Pleistocene and Holocene deposition along the coasts and continental shelves of the Italian peninsula. In: Martini I.P., Vai G.B. (Eds.), *Anatomy of an orogen: the Apennines and adjacent Mediterranean basins*, Kluwer Academic Publishers, Great Britain, 455-478.
- Tortora P., Cowell P.J., Adlam K. 2009. Transgressive coastal systems (1<sup>st</sup> part): barrier migration processes and geometric principles. *Journal of Mediterranean Earth Sciences*: 1, 1-13.
- Wolinsky M.A., Murray A.B. 2009. A unifying framework for shoreline migration: 2. Application to wave-dominated coasts. *Journal of Geophysical Research*: 114, F01009, doi:10.1029/2007JF000856.